© 2014. Published by The Company of Biologists Ltd | The Journal of Experimental Biology (2014) 217, 2221 doi:10.1242/jeb.108175

CORRECTION

Recovery of otoacoustic emissions after high-level noise exposure in the American bullfrog

Dwayne D. Simmons, Rachel Lohr, Helena Wotring, Miriam D. Burton, Rebecca A. Hooper and Richard A. Baird

There was an error published in *J. Exp. Biol.* **217**, pp. 1626-1636.

In Fig. 3, panel A has a duplicated line graph and the keys in panels B and D are incorrect. The correct figure is printed below.

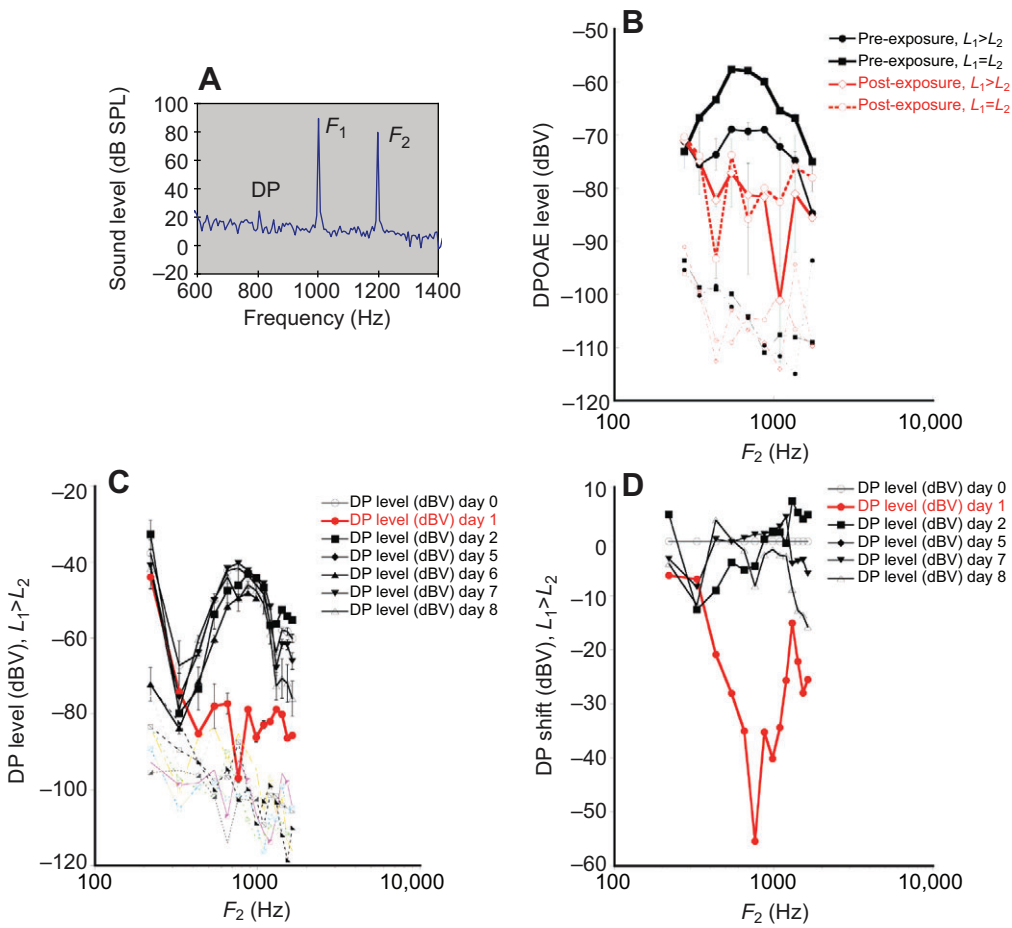

Fig. 3. Cubic distortion products recorded before and after noise exposure in adult bullfrogs. (A) The cubic distortion product (DP) $2f_1–f_2$ recorded from the bullfrog ear with primary f_1 and secondary f_2 frequencies as shown. In this example, secondary levels are 10 dB lower than primary levels. (B) Plot of cubic distortion product otoacoustic emission (DPOAE) levels from the right ear (ipsilateral) versus secondary frequency (f_2). DPOAE levels are in decibels relative to 1 V rms (dBV). The plot depicts DPOAE levels recorded before (solid symbols) and 24 h after (open symbols) 150 dB SPL broad-band noise exposure. Filled and open squares represent corresponding pre- and post-noise levels, respectively. At each frequency, the primary stimulus was held constant at 80 dB SPL and the secondary stimulus level was presented at equal strength (solid squares, L_1=L_2) and then with secondary levels 10 dB lower than primary levels (solid circles, L_1>L_2). Noise level measurements were taken and averaged on either side of the peak DPOAE level immediately before and after noise exposure, with each ear tested and averaged over three presentations. Dashed lines represent noise floor. (C) Cubic DPOAEs (L_1>L_2) from the right ear were tested before (day 0) and 1, 2, 5, 6, 7 and 8 days after noise exposure. Dashed lines represent noise floor. (D) Plot of the DPOAE shifts at each frequency tested before (0 days) and following (1, 2, 5, 6, 7 and 8 days) a 20 h noise exposure. The DPOAE shift was calculated as the difference in pre-exposure and post-exposure DPOAE levels.

We apologise to the authors and readers for this omission.

© 2014. Published by The Company of Biologists Ltd | The Journal of Experimental Biology (2014) 217, 1626-1636 doi:10.1242/jeb.090092

RESEARCH ARTICLE

Recovery of otoacoustic emissions after high-level noise exposure in the American bullfrog

Dwayne D. Simmons[1,*], Rachel Lohr[2], Helena Wotring[2], Miriam D. Burton[2], Rebecca A. Hooper[2] and Richard A. Baird[2]

ABSTRACT

The American bullfrog (*Rana catesbeiana*) has an amphibian papilla (AP) that senses airborne, low-frequency sound and generates distortion product otoacoustic emissions (DPOAEs) similar to other vertebrate species. Although ranid frogs are typically found in noisy environments, the effects of noise on the AP have not been studied. First, we determined the noise levels that diminished DPOAE at $2f_1–f_2$ using an f_2 stimulus level at 80 dB SPL and that also produced morphological damage of the sensory epithelium. Second, we compared DPOAE ($2f_1–f_2$) responses with histopathologic changes occurring in bullfrogs after noise exposure. Consistent morphological damage, such as fragmented hair cells and missing bundles, as well as elimination of DPOAE responses were seen only after very high-level (>150 dB SPL) sound exposures. The morphological response of hair cells to noise differed along the mediolateral AP axis: medial hair cells were sensitive to noise and lateral hair cells were relatively insensitive to noise. Renewed or repaired hair cells were not observed until 9 days post-exposure. Following noise exposure, DPOAE responses disappeared within 24 h and then recovered to normal pre-exposure levels within 3–4 days. Our results suggest that DPOAEs in the bullfrog are sensitive to the initial period of hair cell damage. After noise-induced damage, the bullfrog AP has functional recovery mechanisms that do not depend on substantial hair cell regeneration or repair. Thus, the bullfrog auditory system might serve as an interesting model for investigation of ways to prevent noise damage.

KEY WORDS: Hearing loss, Hair Cells, Regeneration, Cubic distortion product, Active amplification

INTRODUCTION

Anuran amphibians (frogs and toads) live in environments that are inherently noisy at low frequencies, and in which many other frogs of the same species are calling in competition. The sound intensities of frog calls can reach up to 110 dB sound pressure level (SPL) within 50 cm of a calling male frog (Narins and Hurley, 1982). Thus, frogs and toads may have adaptations of their auditory system that facilitate some measure of immunity from the effects of intense sounds and noise-induced hearing loss. Like other vertebrates, the anuran inner ear is a highly sensitive, frequency analyzer. Within the bullfrog inner ear, the amphibian papilla (AP) is a sensor of airborne, low-frequency sound. The AP contains mechanosensitive hair cells that, like the mammalian cochlea, are contacted by the terminal arbors of both afferent and efferent neurons, are tonotopically organized, and generate otoacoustic emissions (OAEs) when tones are given to the ear (reviewed in Simmons et al., 2007). As the by-product of an active amplification process, OAEs in mammals reflect a fundamental property of normal hearing (Kemp, 1978; Kemp, 2002) and provide a non-invasive means of monitoring the active amplification processes necessary for hearing sensitivity (Kössl and Boyan, 1998; Kössl and Vater, 1996; Maison et al., 2007; Shera and Guinan, 1999). One type of OAE that is easily recorded is the distortion product OAE (DPOAE), in which two pure tone stimuli (f_1 and f_2) are presented to the ear and a third difference tone (f_3) is recorded as the cubic distortion product ($2f_1–f_2$). DPOAEs are a sensitive indicator of inner ear integrity and are used routinely for diagnostic screening of inner ear function (Brown et al., 2000; Lonsbury-Martin et al., 1993; Ohlms et al., 1991; Prieve, 2002; Shera and Guinan, 1999). Although DPOAEs initially were thought to be absent in the amphibian ear (Baker et al., 1989), they are now believed to be present in most anuran amphibians (van Dijk and Manley, 2001; Simmons et al., 2007). Some studies suggest that anurans may have both passive and active mechanisms responsible for the generation of DPOAEs (Meenderink and van Dijk, 2006; van Dijk et al., 2011).

In the American bullfrog, *Rana catesbeiana* (*Lithobates catesbeianus*, Shaw 1809), there have been no studies of hair cells after damaging noise levels and no studies of how DPOAEs are affected by noise. The peripheral auditory system of the frog appears designed to minimize the detrimental effects of noisy environments (Carey and Zelick, 1993; Zelick and Narins, 1985; Narins and Zelick, 1988). The bullfrog AP presumably undergoes sensory hair cell repair and regeneration similar to other inner ear organs in the bullfrog (Baird et al., 2000; Gale et al., 2002). If the bullfrog AP does exhibit noise damage, then we would expect the AP to show frequency-specific hair cell loss.

We hypothesized that hair cells in the AP are susceptible to narrow-band noise exposures and should show DPOAE responses that correlate with morphological damage and recovery. Our first goal was to investigate whether the cubic DPOAE ($2f_1–f_2$) was sensitive to noise overexposure. Our second goal was to determine the temporal course of hair cell damage and recovery. This being the first such study of noise-induced hearing loss in the bullfrog, a more detailed understanding of normal AP morphology was also necessitated.

RESULTS

Normal morphology and innervation of the bullfrog AP

In order to assess the effects of noise-induced trauma, we first characterized the normal morphology of the bullfrog AP sensory epithelia. As shown in Fig. 1A, the bullfrog AP has a triangle-shaped, rostral head and a narrower caudal extension. The AP nerve branch approached the sensory epithelium from the lateral side,

[1]Department of Integrative Biology and Physiology, University of California, Los Angeles, 610 Charles E. Young Drive East, Los Angeles, CA 90095, USA.
[2]Central Institute for the Deaf and Washington University School of Medicine, 4560 Clayton Avenue, St Louis, MO 63110, USA.

*Author for correspondence (dd.simmons@ucla.edu)

Received 24 April 2013; Accepted 13 January 2014

The Journal of Experimental Biology

The Journal of Experimental Biology (2014) doi:10.1242/jeb.090092

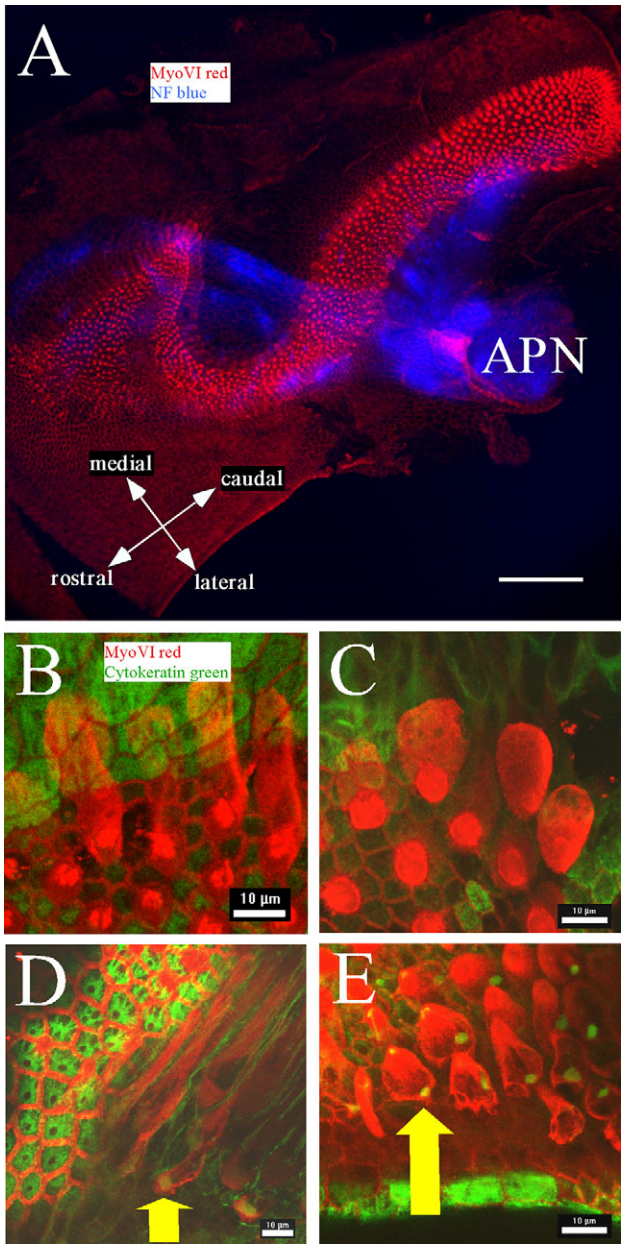

Fig. 1. Overview of bullfrog amphibian papilla. (A) Low-magnification *Z*-projection of a confocal stack of an amphibian papilla nerve branchlet (APN, blue), indicating its bifurcation and approach to the rostral (left) and caudal (right) amphibian papilla (AP). Myosin VI-labeled (MyoVI, red) hair cells extend throughout the rostral and caudal AP. (B–E) *Z*-projections of high-magnification confocal stacks of myosin VI-labeled (red) hair cells and cytokeratin-labeled (green) supporting cells in the rostral (B,D) and caudal (C,E) AP regions. Hair cells located on the medial (B,C) and lateral (D,E) margins of the AP have distinct morphologies. Lateral hair cells (D,E) co-express both myosin VI and cytokeratin (yellow arrows). Scale bars: A, 100 µm; B–E, 10 µm.

bifurcating into two nerve branchlets that pass under and around the sensory epithelium before turning back to innervate hair cells in the rostral or caudal region. Hair cells were homogeneously labeled with myosin VI and supporting cells were labeled with cytokeratin (Fig. 1) (Cyr and Hudspeth, 2000; Cyr et al., 2000). We observed both rostrocaudal and mediolateral morphological differences similar to distinctions previously reported (Lewis, 1976; Lewis, 1984; Lewis and Li, 1975; Shofner and Feng, 1983; Smotherman

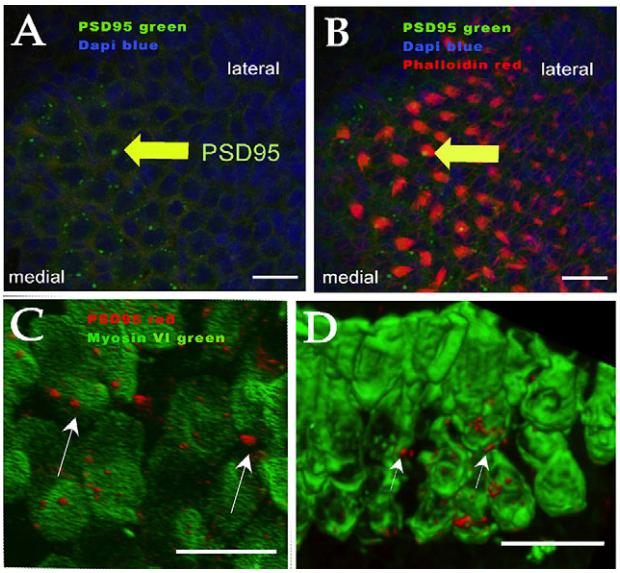

Fig. 2. Immunolabeling of the AP with antibodies against PSD-95. The panels show PSD-95-labeled puncta surrounding hair cells. (A) Low-magnification confocal image showing PSD-95 immunolabeling (green) with DAPI-stained hair cell nuclei (blue). Yellow arrows identify the same PSD-95-labeled puncta in A and B. In both rostral and caudal AP regions, PSD-95 immunoreactivity was especially robust among mature hair cells (on the medial AP margin). (B) Same image as in A except with phalloidin-stained hair bundles (red) to identify hair cells. (C) Higher magnification projection of confocal images of the medial hair cells showing myosin VI-labeled hair cells (green) in caudal medial AP regions. White arrows identify PSD-95-labeled puncta (red) on medial hair cells. (D) Higher magnification reconstruction of myosin VI-labeled hair cells in rostral medial regions of the AP. White arrows identify PSD-95-labeled puncta (red) on medial hair cells. Scale bars represent 10 µm.

and Narins, 2000). In all APs examined (N=20), hair cells along the medial margin had round apical surfaces with uniform hair bundles emerging from circular cuticular plates, and nuclei in the basal third of the sensory epithelium. Rostral hair cells had larger apical surfaces and more elongated cell bodies than hair cells in the caudal extension (Fig. 1B,C). In all cases, hair cells along the lateral edge of both rostral and caudal regions were morphologically distinct. Lateral hair cells had smaller apical surfaces, more lateral hair bundles, and more elongated cell bodies than medial hair cells. We found that these lateral hair cells were also immunocytochemically distinct from hair cells in more medial regions. Hair cells along the lateral margin had myosin VI immunoreactivity but, unlike their more medial counterparts, also expressed cytokeratin in discrete subnuclear clusters (Fig. 1D,E). Three-dimensional reconstructions of lateral hair cells (not shown) clearly demonstrated that cytokeratin labeling was within the hair cell and not in nearby or invading supporting cell processes.

We also immunolabeled excitatory postsynaptic contacts with antibodies against PSD-95. At excitatory synapses, PSD-95 binds NMDA and non-NMDA receptors as well as potassium channels (Craven et al., 1999; Davies et al., 2001; Kornau et al., 1995). Reconstructed confocal images of PSD-95 immunoreactivity surrounding hair cells are shown in Fig. 2. In general, caudal hair cells were contacted by a small number (~5) of large, closely spaced synaptic contacts whereas rostral hair cells were contacted by a greater number (~10) of smaller synaptic contacts. In both rostral and caudal AP regions, PSD-95 immunoreactivity was especially robust among medial hair cells (Fig. 2A,C,D). This

The Journal of Experimental Biology (2014) doi:10.1242/jeb.090092

immunoreactivity is punctate in appearance, forming bead-like plaques that encircle the basolateral portion of the hair cell (Fig. 2A,C,D). Consistent with the presence of afferent terminals on hair cells, PSD-95 immunoreactivity is contained mostly within the subnuclear region of the hair cell and is concentrated at the synaptic terminal region of the hair cell (Fig. 2C,D).

DPOAEs pre- and post-noise exposure

Our goal was to use DPOAEs to monitor both hearing loss and functional recovery and then to compare the recovery of DPOAE levels with morphological recovery. The $2f_1–f_2$ cubic DPOAE was recorded using an earphone and microphone system sealed around the rim of the tympanic membrane (Fig. 3A). In all frogs investigated, DPOAEs at $2f_1–f_2$ (with an f_2/f_1 ratio of 1.2) had stable amplitudes and low variances between re-tests. The f_2 stimulus level was held constant at 80 dB SPL. Equal primary and secondary levels (i.e. $L_1=L_2$) gave the most robust DPOAEs with geometric mean frequencies near 1000 Hz (Fig. 3B). With this stimulus paradigm, DPOAEs above the noise floor could be recorded over a range of secondary (f_2) frequencies from roughly 300 to 1400 Hz. Peak DPOAE amplitudes typically occurred around 800–900 Hz. These DPOAE audiograms had steep DPOAE growth rates on both low- and high-frequency sides. When secondary stimulus levels were 10 dB lower than primary levels (i.e. $L_1>L_2$), DPOAE audiograms differed from those obtained with equal stimulus levels (Fig. 3B). In such cases, DPOAEs above the noise floor were observed over a narrower range of secondary (f_2) frequencies, typically from 500 to 1100 Hz, and peak DPOAE amplitudes were typically 10 dB less for a given f_2 frequency. No DPOAEs were recorded in frogs that died either during the experiment (N=4) or after lethal injections, suggesting that DPOAEs recorded in these frogs are strictly associated with some type of active metabolic processes within the ear.

The biggest differences between equal and unequal stimulus levels occurred in response to noise exposures. Within 24 h of exposure to high-level (>150 dB SPL), 1/3-octave noise bands centered at 800 Hz, equal primary and secondary stimulus levels showed a drop of 10–20 dB in DPOAE amplitude that typically occurred between 500 and 100 Hz (Fig. 3B). Following noise exposure, DPOAE amplitudes were highly variable. This increased variability could be dependent on the depth of anesthesia post-exposure as our goal was frog

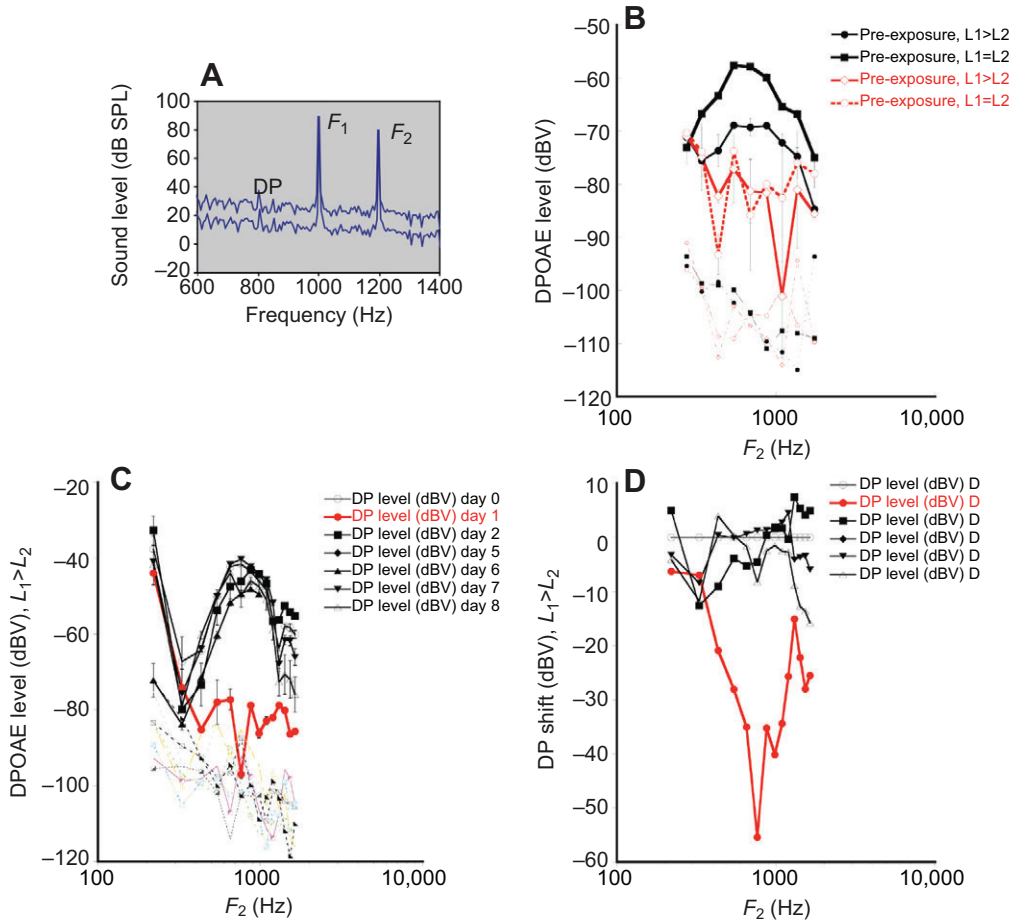

Fig. 3. Cubic distortion products recorded before and after noise exposure in adult bullfrogs. (A) The cubic distortion product (DP) $2f_1–f_2$ recorded from the bullfrog ear with primary f_1 and secondary f_2 frequencies as shown. In this example, secondary levels are 10 dB lower than primary levels. (B) Plot of cubic distortion product otoacoustic emission (DPOAE) levels from the right ear (ipsilateral) versus secondary frequency (f_2). DPOAE levels are in decibels relative to 1 V rms (dBV). The plot depicts DPOAE levels recorded before (solid symbols) and 24 h after (open symbols) 150 dB SPL broad-band noise exposure. Filled and open squares represent corresponding pre- and post-noise levels, respectively. At each frequency, the primary stimulus was held constant at 80 dB SPL and the secondary stimulus level was presented at equal strength (solid squares, $L_1=L_2$) and then with secondary levels 10 dB lower than primary levels (solid circles, $L_1>L_2$). Noise level measurements were taken and averaged on either side of the peak DPOAE level immediately before and after noise exposure, with each ear tested and averaged over three presentations. Dashed lines represent noise floor. (C) Cubic DPOAEs ($L_1>L_2$) from the right ear were tested before (day 0) and 1, 2, 5, 6, 7 and 8 days after noise exposure. Dashed lines represent noise floor. (D) Plot of the DPOAE shifts at each frequency tested before (0 days) and following (1, 2, 5, 6, 7 and 8 days) a 20 h noise exposure. The DPOAE shift was calculated as the difference in pre-exposure and post-exposure DPOAE levels.

The Journal of Experimental Biology (2014) doi:10.1242/jeb.090092

recovery (van Dijk and Manley, 2001). With unequal primary and secondary stimulus levels (i.e. L_1>L_2), there was a consistent, robust drop of at least 20–30 dB with an f_2 frequency between 700 and 1100 Hz (Fig. 3C). This drop in DPOAE amplitude was at or near noise floor levels and demonstrated less variability than those associated with equal primary and secondary levels.

For all subsequent $2f_1$–f_2 DPOAE testing, we used L_2 levels that were 10 dB lower than L_1. We followed DPOAE amplitudes for up to 9 days after intense, high-level, 1/3-octave band noise exposures for 4–24 h. Animals were tested immediately before noise exposure and at varying times following noise exposures. No changes in DPOAE levels occurred with noise exposures that were less than 12 h duration. After longer duration (20–24 h) exposures, DPOAE levels were mostly absent; that is, near the noise floor at an f_2 frequency near 800–1000 Hz (Fig. 3C). Within 3–5 days of exposure, DPOAE levels had recovered to approximate pre-exposure levels (Fig. 3B,C). To compare the changes in DPOAE levels after noise exposure, we calculated the DPOAE shift, i.e. the relative change in DPOAE amplitudes compared with pre-exposure DPOAE amplitudes (Fig. 3D). DPOAE shifts in the exposed (ipsilateral) ear were significantly greater than in the contralateral ear, and the ipsilateral DPOAE amplitude was usually near or at background noise levels. In the contralateral (non-exposed) ear, DPOAE shifts were also present, but highly variable (data not shown). Thus, the contralateral ears could not be used as control ears. In nearly all cases, the maximum DPOAE shift occurred within the first 24–36 h period, suggesting that hair cell function associated with active processes was compromised within that period. DPOAE shifts measured within the first 12 h following noise exposure, although more variable, demonstrated some hypersensitivity before giving a maximum DPOAE shift by 24 h. DPOAE shifts typically returned to pre-exposure levels, suggesting that some type of hair cell recovery occurred within the observed time frame.

We also investigated the relationship between the period of DPOAE recovery and the maximal change in DPOAE amplitude relative to the pre-exposure DPOAE amplitude (maximal DPOAE shift). A plot of the number of animals demonstrating a maximum DPOAE shift (N=11) and recovered DPOAE amplitude (N=16) is shown in Fig. 4A. At 24 h post-exposure, five of 11 animals had a maximal DPOAE shift and none had a recovered DPOAE. By 48 h, nine of 11 animals showed maximal DPOAE shifts and six had recovered DPOAE levels. By 72 h, the remaining two animals had undergone a maximal DPOAE shift and another six animals had recovered. By 96 h, all 16 animals tested had recovered DPOAE amplitudes.

The results presented thus far do not show whether the f_2 frequency input threshold changes after noise exposure. To assess possible changes in the threshold of the f_2 frequency input, the input–output relationship of DPOAE amplitude to f_2 threshold level was determined for five animals. The lowest f_2 level with a recordable DPOAE was taken as the DPOAE threshold. A plot of the relative f_2 threshold and the relative DPOAE threshold is shown in Fig. 4B. When comparing f_2 threshold levels to the pre-exposure f_2 threshold level, four out of five frogs showed an increase in the relative DPOAE threshold level within 12–24 h of noise exposure. By 48 h post-noise exposure all frogs had an f_2 threshold level that intersected with the point at which distortion was measured in our system and, therefore, was not measurable. By 72 h post-noise exposure all five frogs exhibited f_2 threshold levels nearly matching their pre-exposure thresholds. These results suggest that the threshold DPOAE requires increasingly higher stimulus input levels after noise exposure, but recovers relatively quickly after any disruptive effects of the noise have ceased (i.e. by 72 h).

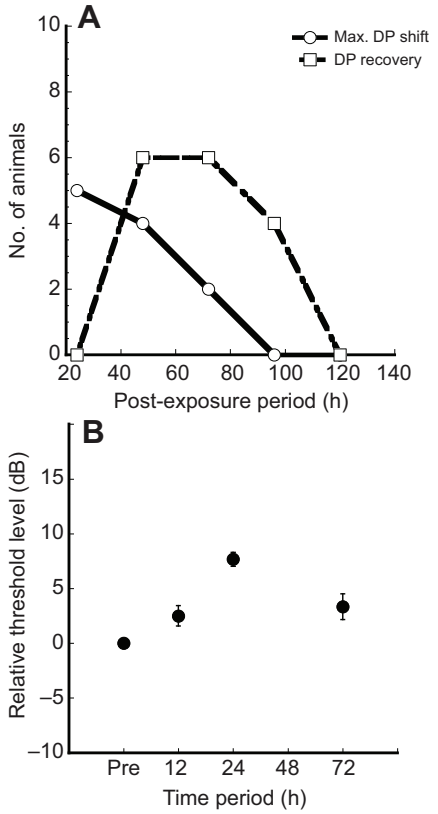

Fig. 4. DPOAE recovery. (A) Plot of the number of animals that have a maximum DPOAE shift (solid line) or have a recovered DP (dashed line) versus the post-exposure period. (B) Plot of the mean relative f_2 threshold level versus time period. The lowest f_2 level with a recordable DPOAE was taken as the threshold and subtracted from the pre-exposure f_2 level threshold. The pre-exposure time period was collected immediately before the noise exposure.

Hair cell damage and recovery

We used pure tone or 1/3-octave frequency bands to investigate whether hair cell damage would be limited to specific regions and to understand the relationship between morphological and functional recovery. After 1/3-octave band noise exposures, we found that noise levels up to 134 dB SPL for durations as long as 24 h were insufficient to cause any significant signs of morphological damage to hair cells (Fig. 5A). Even short duration (4 h) noise exposures up to 150 dB SPL were ineffective at producing observable morphological damage between 12 and 48 h after exposure. However, noise levels of at least 150 dB SPL for 20–24 h caused reproducible damage to hair cells in the bullfrog AP immediately following exposure (Fig. 5B). We therefore exposed the right ears of 33 bullfrogs for 20 h to 150 dB SPL noise bands centered at 800 Hz, and harvested inner ears at 1 day (N=5), 3 days (N=12), 7 days (N=4), 9 days (N=8) or 14 days (N=4) after noise exposure. We observed that hair cells in the caudal AP were severely damaged or lost within 3 days of noise exposure (Fig. 5B). Although there were differences between ipsilaterally exposed ears and contralateral ears, it was clear that caudal hair cells in contralateral ears demonstrated the most hair cell damage. In both ipsilateral and contralateral ears, the most severe damage was always found along the medial margin. We found little, if any, damage to hair cells in lateral AP regions of either ipsilateral or contralateral ears.

Within the first 12–24 h of noise exposure, we observed hair cell damage that included fragmenting hair cells, missing hair cells,

The Journal of Experimental Biology (2014) doi:10.1242/jeb.090092

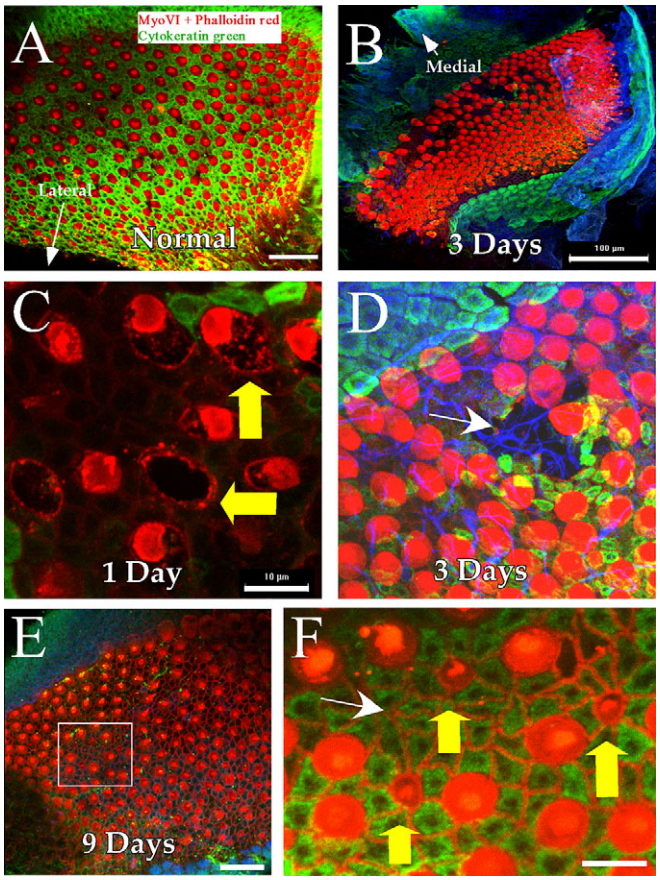

Fig. 5. Noise-damaged AP hair cells. (A–E) Myosin VI-labeled (red) hair cells and cytokeratin-labeled (green) supporting cells in the AP after exposure to noise levels up to 134 dB SPL for 20 h (A) and noise levels at 150 dB SPL for 20 h (B–E). In all panels, the lateral edge is as indicated in A and the medial margin is as indicated in B. Fragmenting hair cells (yellow arrows, C) and epithelial holes (white arrow, D), seen 1 and 3 days after noise exposure, were confined to a narrow region along the medial margin of the caudal region (B). (D–F) Myosin VI- and phalloidin-labeled (red) hair cells and cytokeratin-labeled (green) supporting cells, 3 and 9 days after noise exposure, showing epithelial scar formations (white arrow, F), restoration of intercellular junctions, and the appearance of regenerating hair cells (yellow vertical arrows, F). The box in E is shown at higher magnification in F. Scale bars: 30 µm (A,E); 100 µm (B); 10 µm (C,F). Scale is the same in C and D.

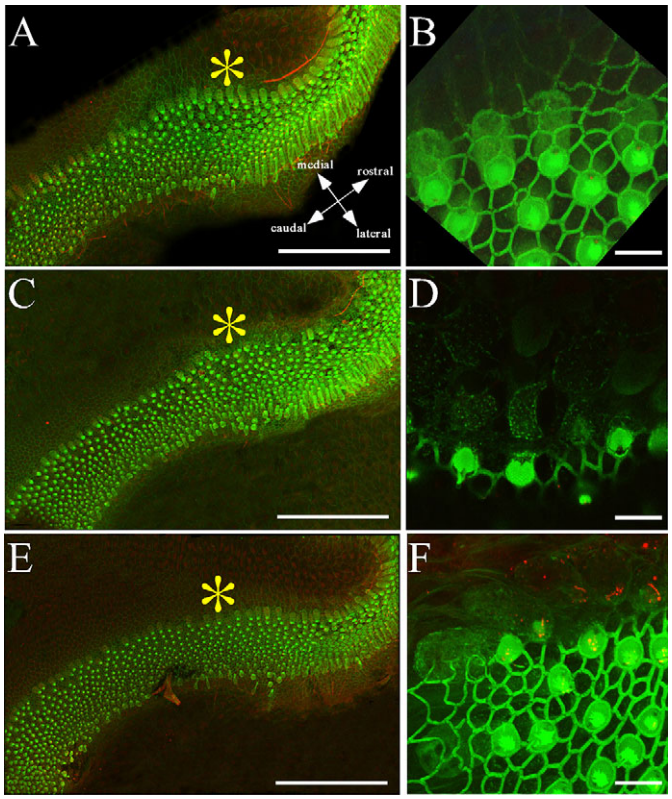

Fig. 6. Hair cell loss in damaged AP regions. Low-magnification (A,C,E) and high-magnification (B,D,F) images of caudal hair cells from normal (A,B) and noise-exposed ears 3 days (C,D) and 9 days (E,F) post-exposure to a high-intensity, 800 Hz tone. Myosin VI and phalloidin are both labeled green. Neurofilament is labeled red. The asterisks represent the same region in each AP as measured from the caudal tail. Regions of epithelial scar formations (S) are also shown. Scale bars: 100 µm (A,C,E) and 10 µm (B,D,F).

reduced cytokeratin labeling in supporting cells and disrupted intercellular junctions (Fig. 5C). We also occasionally observed cytokeratin labeling in hair cells (not shown). Fragmented or spot-like myosin VI labeling was also characteristic of damaged regions 24–72 h after noise exposure (see also Fig. 6D, Fig. 8C,D). In all cases with 1/3-octave band noise, the most dramatic hair cell damage was mostly confined to the medial margin of the caudal extension (roughly 800–1000 Hz region) while moderate damage extended toward the rostral region up to the caudal tail neck region (roughly the 500–600 Hz region) but was never seen in the rostral head. Missing hair cells were replaced by epithelial scar formations within 72 h (Fig. 5D). Scar formations consisted of an actin mesh network of four to eight polygonal epithelial cells. These formations are likely created by the expansion of the apical projections of neighboring epithelial cells into the epithelial spaces vacated by hair cells (Baird et al., 2000). Hair cells located in more lateral regions adjacent to the lateral margin sometimes had splayed hair bundles but no obvious signs of missing or otherwise damaged hair cells, suggesting that they were more resilient to noise damage. Recovery was evident along the medial margin 9 days after noise exposure, which included, for example, the restoration of intercellular junctions (Fig. 5E). At 9 days, numerous repairing or regenerating hair cells had immature hair bundles (Fig. 5F).

We documented hair cell loss in response to a pure tone in five normal (unexposed) ears and seven experimental ears following 20 h exposure to an 800 Hz stimulus at 150 dB SPL. As revealed by anti-myosin VI and phalloidin staining (both green) in Fig. 6A, unexposed ears had little evidence of hair cell loss as defined by the absence of a cuticular plate or disruption to the regularly arrayed (polygonal) mesh network interspersed between myosin VI-labeled hair cells. Fig. 6C,D and 6E,F show AP organs 3 and 9 days following noise exposure. In general, 800 Hz exposures produced regions of damage that were more narrowly confined than 1/3-octave band noise exposures. At 3 days, many hair cells within the region of damage had swollen and/or fragmented cell bodies, abnormal apical surfaces and some missing cuticular plates (Fig. 6D). There was also an increase in the presence of epithelial scar formations. At 9 days, hair cells in the damaged regions had nearly normal myosin VI immunolabeling, normal appearing cuticular plates and hair bundles of varying sizes. Unlike the normal AP, damaged regions had increased scar formations (Fig. 6F) that gave rise to the appearance of a lower density of hair cells, suggesting evidence of hair cell loss.

The Journal of Experimental Biology (2014) doi:10.1242/jeb.090092

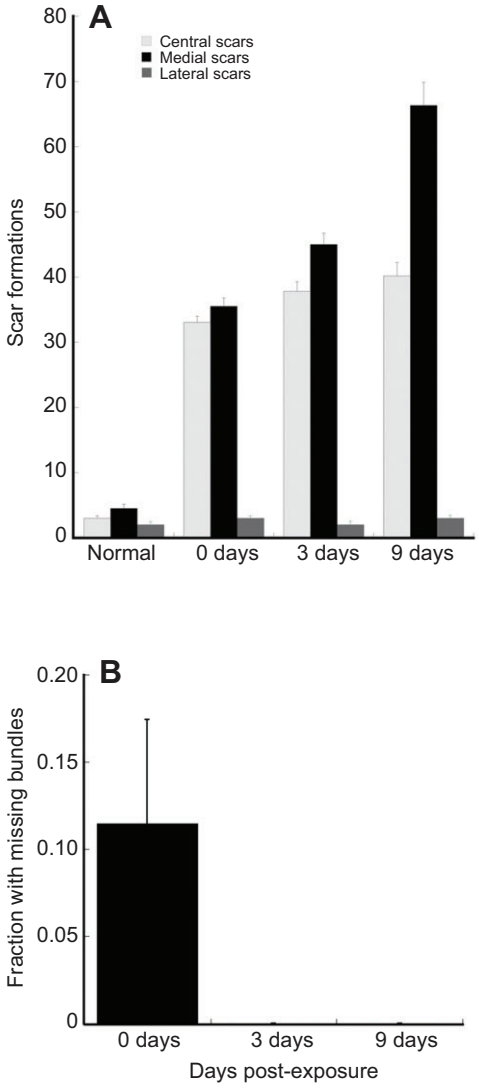

Fig. 7. Epithelial scars and missing hair bundles. (A) The number of epithelial scars was plotted in normal ears and exposed ears after 0, 3 and 9 days. Epithelial scars were counted in 100 µm distance bins from the end (tip) of the caudal extension of an exposed ear and non-exposed ear from the same animal. (B) The fraction of hair cells with missing bundles was plotted in exposed ears after 0, 3 and 9 days. Only mature hair cells in exposed ears showed a significant number of missing stereocilia bundles.

It was difficult to assess directly hair cell loss at different periods of recovery because of their irregular organization. We divided the caudal AP into 100 µm distance bins along the rostrocaudal axis. Furthermore, we divided hair cells into three radial groups – medial, central and lateral – primarily on the basis of location but also because of other characteristics such as cell body and bundle morphology. The number of missing medial and central hair cells was then approximated by counting the number of medial margin, central and lateral scar formations in the 100 µm distance rostrocaudal bins of normal control (N=5) ears and exposed ears within the first 12–24 h (0 days, N=9), 3 days (72 h, N=4), and 9 days (N=3) of noise exposure. As expected from our observations of hair cell damage, the number of medial scars was highest and the number of lateral scars lowest and virtually unchanged in exposed ears compared with control normal ears (Fig. 7A). At 0 days after exposure, the number of medial scars was not much different from the number of central scars, but both were greater than in control ears. At 3 days after exposure, the number of scars increased, with a slightly higher number in medial margin regions. By 9 days after exposure, the number of medial scars was highest. There were no other obvious signs of damage apart from a few splayed hair bundles in lateral hair cells.

As active processes in non-mammalian vertebrates may involve the hair bundle, the number of hair cells with missing bundles was also plotted against caudal extension position for medial margin hair cells (Fig. 7B). We did not observe any central or lateral hair cells with missing hair bundles; therefore, our data are restricted to medial margin hair cells. In control ears, no medial hair cells were found with missing hair bundles. Twenty-four hours after noise exposure, hair cells with missing hair bundles were found in about half of the experimental cases and these hair cells were limited to the medial margin throughout the caudal extension. However, the number of medial hair cells with missing hair bundles was highly variable across animals. By 3 days after noise exposure, no medial margin hair cells were found with missing bundles anywhere in the caudal extension. There are at least two explanations for the absence of hair cells with missing bundles: either these hair cells repaired or re-grew their hair bundles or the hair cells without bundles were no longer present.

Qualitative observations on synaptic recovery

We made qualitative observations as to the extent of synaptic recovery after 0, 1, 3, 9 or 14 days post-exposure survival. First, three bullfrogs, were given high-intensity (150 dB SPL), 1/3-octave band (cf. 800 Hz), short duration (4 h) noise exposures in one ear. Compared with the contralateral ear (Fig. 8A), the right exposed ears all demonstrated an increase in PSD-95 immunoreactive puncta within the first 24 h (Fig. 8B). Longer (20–24 h) high-intensity noise exposures produced secondary, severe morphological disruption to neurofilament-labeled fibers, resulting in fewer PSD-95 immunoreactive puncta in the damaged regions (Fig. 8C). At 3 days post-exposure, although myosin VI-labeled hair cells were missing in damaged regions, PSD-95 labeled profiles were observed that co-localized with myosin VI fragments representative of this post-exposure stage (Fig. 8D). Such myosin VI and PSD-95 fragments were not associated with synaptic endings, suggesting that many synaptic connections were disrupted by the noise stimulus. At 9 days post-exposure, the luminal surface was completely repaired with newly generated hair cells present (Fig. 8E). Although afferent re-innervation of the damaged region was not complete by 9 days, a decrease in isolated PSD-95 and co-localized myosin VI and PSD-95 fragments were seen (Fig. 8F). By 14 days after sound exposure, regenerating medial hair cells in the damaged region were contacted by thin neurofilament-labeled fibers and had small PSD-95-labeled puncta (Fig. 8G–I).

DISCUSSION

The present study is the first to investigate high-intensity noise exposure in the bullfrog. The bullfrog AP requires long-term (20–24 h), high-level (>150 dB SPL) noise exposures in order to produce consistent damage of the sensory epithelium and maximal DPOAE shifts. Significantly, we found that morphological recovery and physiological recovery from overexposure to noise are not synchronized. Additionally, our results not only extend previous findings of morphological differences across the bullfrog AP mediolateral axis but also suggest that these morphological differences correlate with differences in sensitivity to acoustic trauma. High-intensity, narrow-band sound produces morphological damage concentrated along the medial margin of the bullfrog caudal

The Journal of Experimental Biology (2014) doi:10.1242/jeb.090092

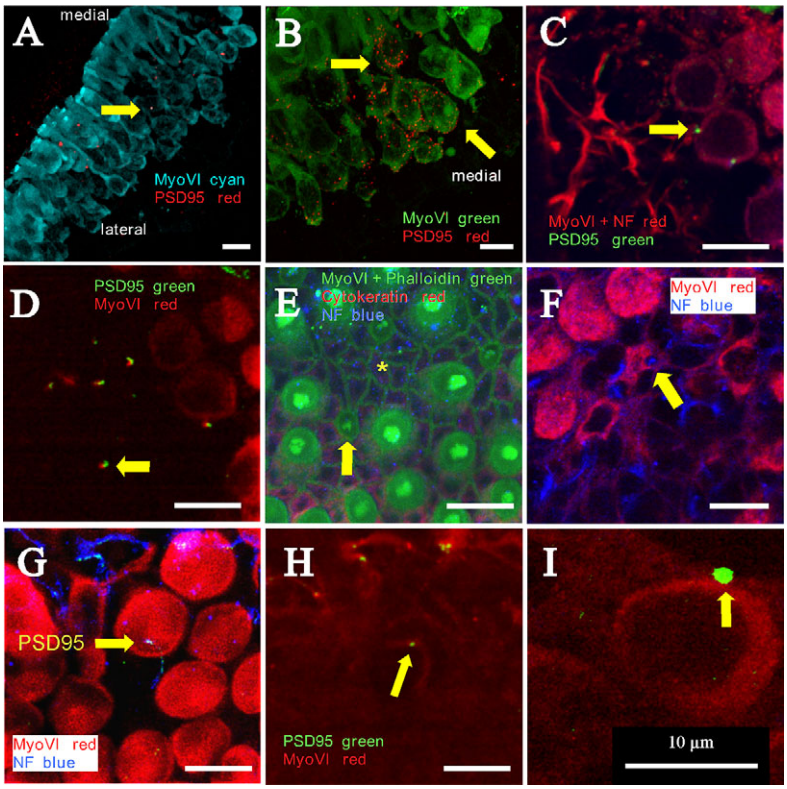

Fig. 8. PSD-95 and neurofilament labeling after noise exposure. (A) An unexposed control AP labeled with myosin VI (blue) and PSD-95 (red). PSD-95 puncta (yellow arrow) are found on medial hair cells and not lateral hair cells. (B) After a short (4 h) noise exposure (150 dB SPL), PSD-95 immunoreactivity (red) dramatically increases on medial hair cells. AP hair cells are labeled with myosin VI (green). Yellow arrows identify PSD-95 puncta surrounding the basolateral portions of hair cells. (C) Myosin VI-labeled hair cells (red), PSD-95 labeled puncta (green) and neurofilament (NF) labeled fibers (red) 1 day after a 20 h noise exposure. Yellow arrow identifies PSD-95 puncta apposed to a myosin VI-labeled medial hair cell. (D) Myosin VI-labeled hair cells (red) and PSD-95 labeled puncta (green) 3 days after a 20 h noise exposure. Yellow arrow shows PSD-95 puncta overlapping with myosin VI-labeled fragment. (E) Luminal surface view of myosin VI- and phalloidin-labeled hair cells (green) 9 days after a 20 h sound exposure, showing restoration of scars and intercellular junctions (asterisk), and the appearance of regenerating hair cells (yellow arrow). (F) A view near the basement membrane of a sound-exposed caudal AP 9 days after sound exposure. Myosin VI-labeled hair cells (red) are contacted by neurofilament-labeled (blue) fibers (yellow arrow). (G) Recovered hair cells 14 days after sound exposure. This region of the AP has new connections from neurofilament-labeled (blue) auditory neurons (yellow arrow). (H) At 14 days after sound exposure, punctate PSD-95 immunoreactivity (yellow arrow) was also seen closer to the basement membrane within scar formations. (I) Higher magnification image of a myosin VI-labeled hair cell (red) from H showing punctate PSD-95 immunoreactivity (green; yellow arrow) by 14 days post-sound exposure. All scale bars represent 10 µm.

AP. The finding that the bullfrog AP regenerates hair cells following acoustic trauma could make it an attractive model in which to study noise damage after high-level noise exposures.

Our results confirm that the most robust DPOAEs at $2f_1–f_2$ are near 800 Hz. The greatest DPOAE shift following noise exposure was located in regions consistent with maximal $2f_1–f_2$ responses. The complete abolishment of the DPOAE required the delivery of a very intense signal (≥150 dB SPL) to the ear for 20 h. Our data suggest that in the bullfrog, DPOAE levels are sensitive to hair cell damage. However, DPOAEs showed partial, if not full, recovery of their original amplitude as early as 72 h after noise exposure. Although DPOAEs recover within 3–5 days of sound exposure, morphological recovery was not complete until after 9 days. The time course between DPOAE and morphological recovery illustrates a potentially significant dissonance between these morphological and physiological parameters. If the high stimulus level DPOAE used in this study is generated from passive non-linear responses from the caudal AP (Meenderink and van Dijk, 2004), it may explain the observation that they return to normal levels before full morphological recovery of the caudal hair cells. Although the recorded DPOAEs may be passively generated, the observations that they were sensitive to animal viability also suggests that they are associated with some type of active metabolic process.

Our data raise the possibility that there may be multiple functional populations of hair cells in bullfrogs reminiscent of the hair cell dichotomy seen in the bird and mammal cochlea. Hair cells along the medial margin of the caudal AP not only are more susceptible to noise trauma but also receive an afferent innervation characterized by PSD-95 immunoreactivity and lack any cytokeratin immunoreactivity. Amphibian papillar hair cells in more lateral locations are less sensitive to noise trauma, have little PSD-95 immunoreactivity and show cytokeratin immunoreactivity. Intense, but relative short duration, noise stimulation in the bullfrog does not produce any severe morphological trauma but does increase the amount of PSD-95 immunoreactivity observed in medial hair cells. Longer duration traumatic noise stimulation obliterates myosin VI labeling of medial hair cells and disrupts cytokeratin labeling in supporting cells reminiscent of recent studies after noxious insult in the bullfrog sacculus (Hordichok and Steyger, 2007). Previous studies suggest that cytokeratin expression may be downregulated during hair cell differentiation (Cyr et al., 2000). In the present study, however, cytokeratin regulation may be associated with mechanisms of cell death and/or sensory repair in which the sensory epithelium is attempting or preparing for recovery (Hordichok and Steyger, 2007). PSD-95 fragments also remain associated with myosin VI-labeled fragments of hair cells in damaged regions. Even after major hair cell damage, afferent nerve terminals may still be present and may be ready to re-innervate new hair cells. At least one other study has shown that levels of PSD-95 are associated with sound-evoked activity (Bao et al., 2004).

There have been surprisingly few studies of the afferent innervation of regenerated hair cells (Duckert and Rubel, 1990; Duckert and Rubel, 1993; Haque et al., 2009; Ryals and Westbrook, 1994; Xiang et al., 2000; Zakir and Dickman, 2006). New synaptic endings are seen on repairing and regenerating hair cells soon after their appearance, but normal innervation is not restored for much longer periods (Haque et al., 2009; Ryals and Westbrook, 1994; Whitlon and Sobkowicz, 1991; Zakir and Dickman, 2006). Rapid functional recovery after sound trauma may be associated with processes involving the surviving hair cells – rather than with the regeneration of lost hair cells (Reng et al., 2001). This idea would be consistent with the present results in the bullfrog. However, in the bird cochlea, after ototoxic trauma, functional recovery is typically slower and parallels the structural regeneration more closely. The completeness of functional recovery also differs according to frequency, with regions of higher frequencies demonstrating more incomplete functional recovery (Cotanche, 1999).

OAEs and hair bundles

Our study is the first to investigate DPOAE shifts in response to noise exposure in the frog. Previous studies of the effects of noise on the auditory system of frogs have been limited mostly to observations of temporary threshold shifts of auditory nerve responses (e.g. Zelick and Narins, 1985). The DPOAEs recorded in this study displayed sensitivity and amplitude patterns consistent with the findings of other researchers. van Dijk and Manley recorded DPOAE amplitudes ranging from ~5 to 15 dB SPL (van Dijk and Manley, 2001), similar to the findings of Meenderink et al., who reported average DPOAE amplitudes of ~5 dB SPL (Meenderink et al., 2005). Maximum DPOAE amplitudes were recorded at DPOAE frequencies ranging from ~600 to 1000 Hz, corresponding to our finding that an f_2 frequency of 800–1200 Hz elicits the most robust response (Meenderink et al., 2005; Simmons et al., 2007; van Dijk and Manley, 2001; Vassilakis et al., 2004).

Based on theoretical and experimental work in mammals and humans, it is widely accepted that the DPOAE at $2f_2–f_1$ can be interpreted as the sum of two frequency components: a distortion component originating close to f_2 and a reflection component originating at the site of the distortion product, $2f_2–f_1$ (Shera and Guinan, 1999; Mauermann and Kollmeier, 2004). In mammals, the DPOAE input/output function can be used to characterize changes in cochlear non-linearity or for the prediction of thresholds (Mauermann and Kollmeier, 2004; Mills, 2004). In five frogs, we observed that the f_2 levels necessary to obtain a DPOAE threshold increased following noise exposure similar to predictions in mammals with hearing loss. Increasing f_2 levels could be indicative of damage to the distortion component, and consistent with DPOAEs in the frog also having two frequency components.

In amphibians, reptiles and birds, the best candidate for an active process may be the active motility of mechanically sensitive hair bundles (Bozovic and Hudspeth, 2003; Fettiplace, 2006; Hudspeth et al., 2000). In the present study, DPOAE recovery in bullfrogs is better correlated with the number of intact hair bundles than with the number of repairing/regenerating hair cells, suggesting that DPOAEs require intact hair bundles and may be linked to hair bundle micromechanics. Many studies have shown that repairing and regenerating hair cells develop normal-appearing hair bundles and seem functional. The first suggestion that damaged hair cells could repair their bundles was based on observations of hair cell recovery in cultures of neonatal mice organ of Corti (Sobkowicz et al., 1993). Laser-damaged hair cells also appear to re-grow their stereociliary bundles once they regain contact with the luminal surface (Sobkowicz et al., 1997). Hair cells in damaged vestibular organs appear to restore their hair bundles through a process of self-repair (Gale et al., 2004; Zheng et al., 1999).

The suggestion that intact hair bundles may be associated with the presence or absence DPOAEs is also consistent with studies of the mammalian cochlea using prestin-null mice (Cheatham et al., 2004; Dallos et al., 2008; Liberman et al., 2004). Without prestin, outer hair cells are incapable of electromotility, thus eliminating outer hair cell somatic motility as a dominant source of DPOAE generation. Liberman et al. (Liberman et al., 2004) attributed the continued presence of DPOAEs at high stimulus levels to the fast adaptation of outer hair cell stereocilia bundles as they appeared to be the only non-linearity left within the organ of Corti. In mice and chinchillas, damage to supporting cells and the uncoupling of stereocilia are also better predictors of DPOAE shift than the presence of outer hair cells (Harding and Bohne, 2004a; Harding and Bohne, 2004b). There is increasing evidence that in non-mammalian vertebrates, active movements of hair bundles are necessary for amplification and thus the generation of otoacoustic emissions (Fettiplace, 2006; Peng and Ricci, 2011).

In this study, we measured DPOAEs using relatively high-level stimuli (80 dB SPL). Previous investigations in the frog have interpreted DPOAEs resulting from such high-level stimuli as representing a passive non-linearity in the frog's auditory epithelia. This interpretation is based on the fact that these high-level components are insensitive to body temperature changes (Meenderink and van Dijk, 2006) and persist post mortem (van Dijk et al., 2003). The observation that these DPOAEs were abolished over a similar time course to morphological damage argues that they are associated somehow with the morphological integrity of the AP and, in particular, caudal hair bundles. Furthermore, the DPOAEs recorded in this study did not persist post mortem. Therefore, our data are consistent with the idea that the source of DPOAEs produced at high stimulus levels prior to noise exposure may be associated with the non-linear mechanics of the stereocilia bundle in active hair cells and noise disrupts this function. However, our data do not address whether the source of the recovered DPOAEs is associated with active or passive mechanics of the hair bundle. As mentioned previously, the apparent dissociation between DPOAE recovery and morphological recovery suggests that the recovered DPOAE is not dependent on total hair cell recovery. It is tempting to speculate that the recovered DPOAE is generated from the hair bundles associated with either more lateral hair cells or remaining undamaged medial hair cells.

In conclusion, frogs typically are located in environments with intense, broad spectrum, ambient noises and therefore have derived multiple solutions to maximize audible signal throughput (Feng et al., 2006; Narins and Wagner, 1989; Narins et al., 1988). We had to use extremely high-intensity sound levels to induce hearing loss. Our results indicate that the processes that generate the $2f_1–f_2$ DPOAE at high stimulus levels are highly resilient to high-intensity noise, and that the $2f_1–f_2$ DPOAE recovers much faster than the parameters typically associated with morphological recovery would suggest. We speculate that the $2f_1–f_2$ DPOAE is capable of being generated from multiple sources across the sensory epithelium that allow it to return quickly after traumatic insult.

MATERIALS AND METHODS

Animals

Adult bullfrogs, *R. catesbeiana* (measuring 102 mm, snout to vent length), were obtained from Carolina Biological Supply (www.carolina.com) and housed in fresh, de-chlorinated water in large recirculating aquaria according to published standards of the US Public Health Service. Bullfrogs were anesthetized for a minimum of 20 min in 0.2% tricaine methanesulfonate (MS-222) for all *in vivo* procedures, and killed by decapitation. For sound experiments, a single intramuscular dose of sodium pentobarbital (50 mg kg^{-1} body mass) was given. All experimental procedures were approved by the animal committees at Washington University School of Medicine and the University of California, Los Angeles.

In vivo sound exposure

Noise stimuli were delivered via a closed acoustic system. After 20 min in 0.2% MS-222, either left or right ears of bullfrogs were exposed for 4 or 20 h to high-intensity (150–160 dB) pure tone at 800 Hz or 1/3-octave noise bands centered at 800 Hz to eliminate DPOAEs and damage hair cells in the caudal amphibian papilla. To prevent dehydration, animals were kept moist by constant application of Ringer's solution with 0.1% MS-222. An Altec 802D horn driver with a flexible 3/8 in (9.5 mm) i.d. hard wall vinyl tube delivered low-frequency pure tones or 1/3-octave noise bands centered at 800 Hz to the bullfrog ear tympanic membrane [~1/4 in (6.4 mm) diameter] using a pure tone generator and 60 W power amplifier. We continuously measured the driver output at a side tube extension of the horn driver with a 4134 Bruel and Kjaer microphone. In order to not damage the tympanic

Table 1. Antibody inventory used to investigate hair cells and synapses in the amphibian papilla

Target	Manufacturer (product no.)	Immunogen	Host	Working dilution	Positive control	Negative control
Myosin VI	Sigma (KA-15)	Human myosin VI (C-terminal)	Rabbit	1:100	Manufacturer's immunoblotting	Omission of 1° Ab
Myosin VI	Proteus (25-6791)	Porcine myosin VI (aa 1049–1254)	Rabbit	1:100	{Hasson:1997tx}	Omission of 1° Ab
Calbindin	Swant (CB38)	Recombinant rat calbindin D-28k	Rabbit	1:250	Immunohistochemistry on cerebellum sections	Omission of 1° Ab
Calbindin	Swant (300)	Calbindin D-28k, purified from chicken gut	Mouse (mAb)	1:250	Immunohistochemistry on cerebellum sections	Omission of 1° Ab
Cytokeratin	Gift from Dr J. Cyr, University of West Virginia School of Medicine	Bactiophage antibody fragment library of bullfrog inner ear proteins	Mouse (mAb)	1:20	{Cyr:2000jz}	Omission of 1° Ab
PSD-95	BD Transduction Laboratories (610495)	Rat PSD-95 (aa 353–504)	Mouse (mAb)	1:100	Manufacturer's western blot rat brain	Omission of 1° Ab

1° Ab, primary antibody; mAb, monoclonal antibody; aa, amino acids.

membrane or impede sound transmission, a latex rubber tip was loosely sealed with silicone onto the rim of the tympanic membrane.

Sound exposures lasted 20–24 h in order to produce consistent damage. With this setup we delivered ~150–160 dB SPL without significant distortion between 600 and 1600 Hz. A driver output of 158.0 dB SPL at 800 Hz produced 159.8 dB SPL at the latex rubber tip. Right and left ears were acoustically decoupled to minimize intra-oral interactions.

DPOAE measurements

Equipment was calibrated using a 2231 type Bruel and Kjaer sound level meter with a 0.5 in (12.7 mm) pressure microphone in a Zwislocki coupler. Stimulus intensities were calibrated in a 0.5 cc cavity using a sound level meter (A-weighting frequency filter). Stimulus responses were averaged 100–200 times. The biologic signal was amplified (×100,000) and notch filtered at 60 Hz with a DB4 Digital Biological Amplifier (Tucker-Davis Technologies, TDT, Alachua, FL, USA) during data collection. The signal was band-pass filtered below 30 Hz and above 3000 Hz after collection using the TDT BioSig program. Cubic DPOAEs at $2f_1$–f_2 were recorded through a low-noise ER10C earphone (Etymotic Research, Elk Grove, IL, USA) and microphone system placed around the bullfrog's tympanic membrane using TDT hardware and software to generate stimulus tones. DPOAE levels were expressed in decibels relative to 1 V rms (dBV). The primary (f_1) and secondary (f_2) stimulus frequencies were determined from geometric mean frequencies (Hz) centered at 250, 311, 394, 494, 628, 794, 994, 1239 and 1589 Hz with the frequency ratio (f_2/f_1) set to 1.2. At each frequency, stimulus levels were first presented with constant (80 dB SPL) equal primary and secondary levels (i.e. L_1=L_2) and then with secondary levels being 10 dB lower than the primary level (i.e. L_1=90 dB SPL and L_2=80 dB SPL). Noise level measurements were taken and averaged on either side of the peak DPOAE level immediately before and after noise exposure, with each ear tested and averaged over three presentations.

DPOAE measurements were taken immediately before noise exposure and 12, 24, 48 and 72 h post-noise exposure, or until DPOAE recovery. Using an f_2 stimulus level at 80 dB SPL, three measurements were averaged at each frequency. We also recorded the lowest f_2 level with a recordable DPOAE, which was taken as the DPOAE threshold. Once DPOAE recovery was observed at $2f_1$–f_2, the animal was killed and the ears were collected and prepared for confocal microscopy. To determine the non-linear distortion of the recording system, the probe was placed against a solid surface after each measurement session. No distortion was noted at any of the threshold levels where a DPOAE was recorded. This process was crosschecked by performing pre- and post-death DPOAE measurements on a frog. No non-linear distortion was noted where DPOAEs had been recorded pre-death.

Dissection of the bullfrog AP

After an appropriate post-exposure survival period (0, 1, 3, 9 or 14 days), we re-anesthetized and decapitated noise-exposed bullfrogs, dissecting their APs in chilled, oxygenated Hepes-buffered saline (HBS) containing (mmol l^{-1}): 110 Na^+, 2 K^+, 4 Ca^{2+}, 120 Cl^-, 3 D-glucose and 5 Hepes, pH 7.25. We then transferred APs to amphibian phosphate-buffered saline (PBS) for subsequent experiments. For immunocytochemistry, AP tissues were fixed in 4% paraformaldehyde, permeabilized in 0.5% Triton X-100 in PBS to enhance antisera penetration, and incubated in a blocking solution consisting of 3% normal horse serum and 1% BSA in PBS to reduce non-specific labeling. Some ears were embedded in gelatin–agarose and sectioned at 200 μm on a Vibratome.

Immunocytochemistry

The antibodies used to characterize hair cells, support cells, nerve fibers and synapses are listed in Table 1. Included in this table are the specifications for the immunogen, the host in which it was raised, and controls. Tissues were immunolabeled with various combinations of antisera against either myosin VI or calbindin D-28k to label hair cells, inner ear cytokeratin to label supporting cells and PSD-95 to label synapses. We confirmed myosin VI and calbindin D-28k immunolabeling by comparing cellular labeling using two different primary antisera. For double- and triple-immunolabeling experiments, primary antisera from different species were often incubated together. APs were incubated overnight at 4°C in a primary antisera cocktail diluted in PBS. APs were then incubated in fluorescently conjugated secondary antisera [such as CY5-conjugated GAR IgG (Americium, GE Health Sciences, Piscataway, NJ, USA), biotinylated HAM IgG (Vector Laboratories, Burlingame, CA, USA) or Alexa 594 streptavidin (Molecular Probes, Life Technologies, Carlsbad, CA, USA)]. After secondary antibody labeling, tissues were stained with DAPI to label cell nuclei and Alexa-conjugated phalloidin (0.2%) to label hair bundles. Tissue was then mounted in Fluoromount (Southern Biotechnology, Birmingham, AL, USA) and examined with confocal microscopy. Negative controls, including the omission of primary antisera and substitution of normal serum for primary antisera were used. We pre-tested all antisera for specificity and sensitivity in single labeling experiments before using them in multiple labeling experiments.

Confocal microscopy

We used green (Alexa 488), red (Alexa 594) and far-red (Alexa 647/660) fluorophores, a combination that minimized spectral bleed-through between adjacent channels, to triple-label APs. Using a laser scanning confocal microscope (Zeiss LSM 5 or Bio-Rad Radiance 2000 AGR-3, Thornton, NY, USA) and a ×60 water-immersion (NA=1.20) objective (Plan Apochromat, Nikon), inner ear sensory organs were visualized and reconstructed. Fluorescent emissions were simultaneously acquired with appropriate blocking and emission filters, scanned at slow (25–50 lines s^{-1}) scan speeds for maximum resolution, and independently detected with either 8- or 12-bit accuracy by photomultiplier tubes. 3D images of serially reconstructed image stacks from the confocal microscope were rendered using Velocity (v4.xx; Improvision, PerkinElmer, Shelton, CT, USA). *Z*-projections of images were routinely performed.

Single confocal images were de-convolved to remove out-of-focus information and median filtered to eliminate image noise, and gray levels were adjusted from the stack histogram to maximize brightness and contrast (MicroTome, VayTek, Fairfield, IA, USA; Velocity, PerkinElmer). We applied a constrained iterative deconvolution algorithm with a measured point-spread function to confocal image stacks. We then reconstructed and rendered hair cells in de-convolved image stacks using 3D image rendering programs (Volocity, PerkinElmer; NeuroLucida, MicroBrightField, Williston, VT, USA).

Acknowledgements
The authors acknowledge the generous gift of recombinant antibody against inner ear cytokeratin from Drs A. J. Hudspeth and J. Cyr and technical support from Saori Yonebayashi and Aubrey Hornak.

Competing interests
The authors declare no competing financial interests.

Author contributions
D.D.S. designed experiments, assisted with hearing tests, performed immunocytochemical experiments, did confocal microscopy, analysed data, and wrote and edited the manuscript. R.L. performed hearing tests, analysed data, and helped write the manuscript. H.W. performed hearing tests and helped with data analysis. M.D.B. helped with experimental design, performed immunocytochemical experiments and did confocal microscopy. R.A.H. performed immunocytochemistry and image analysis. R.A.B. helped with experimental design and helped write the manuscript.

Funding
The National Institutes of Health [DC004086 to D.D.S. DC00240 to R.A.B.] and National Aeronautics and Space Administration [NCC 2–651 to R.A.B.], and UCLA Department of Integrative Biology and Physiology supported this work. Deposited in PMC for release after 12 months.

References

Baird, R. A., Burton, M. D., Lysakowski, A., Fashena, D. S. and Naeger, R. A. (2000). Hair cell recovery in mitotically blocked cultures of the bullfrog saccule. *Proc. Natl. Acad. Sci. USA* **97**, 11722-11729.
Baker, R. J., Wilson, J. P. and Whitehead, M. L. (1989). Otoacoustic evidence for nonlinear behavior in frog hearing: suppression but no distortion products. In *Cochlear Mechanisms: Structure, Function and Models* (ed. J. Wilson and D. T. Kemp), pp. 349-356. New York, NY: Plenum.
Bao, J., Lin, H., Ouyang, Y., Lei, D., Osman, A., Kim, T.-W., Mei, L., Dai, P., Ohlemiller, K. K. and Ambron, R. T. (2004). Activity-dependent transcription regulation of PSD-95 by neuregulin-1 and Eos. *Nat. Neurosci.* **7**, 1250-1258.
Bozovic, D. and Hudspeth, A. J. (2003). Hair-bundle movements elicited by transepithelial electrical stimulation of hair cells in the sacculus of the bullfrog. *Proc. Natl. Acad. Sci. USA* **100**, 958-963.
Brown, D. K., Bowman, D. M. and Kimberley, B. P. (2000). The effects of maturation and stimulus parameters on the optimal f(2)/f(1) ratio of the 2f(1)-f(2) distortion product otoacoustic emission in neonates(1). *Hear. Res.* **145**, 17-24.
Carey, M. B. and Zelick, R. (1993). The effect of sound level, temperature and dehydration on the brainstem auditory evoked potential in anuran amphibians. *Hear. Res.* **70**, 216-228.
Cheatham, M. A., Huynh, K. H., Gao, J., Zuo, J. and Dallos, P. (2004). Cochlear function in Prestin knockout mice. *J. Physiol.* **560**, 821-830.
Cotanche, D. A. (1999). Structural recovery from sound and aminoglycoside damage in the avian cochlea. *Audiol. Neurootol.* **4**, 271-285.
Craven, S. E., El-Husseini, A. E. and Bredt, D. S. (1999). Synaptic targeting of the postsynaptic density protein PSD-95 mediated by lipid and protein motifs. *Neuron* **22**, 497-509.
Cyr, J. L. and Hudspeth, A. J. (2000). A library of bacteriophage-displayed antibody fragments directed against proteins of the inner ear. *Proc. Natl. Acad. Sci. USA* **97**, 2276-2281.
Cyr, J. L., Bell, A. M. and Hudspeth, A. J. (2000). Identification with a recombinant antibody of an inner-ear cytokeratin, a marker for hair-cell differentiation. *Proc. Natl. Acad. Sci. USA* **97**, 4908-4913.
Dallos, P., Wu, X., Cheatham, M. A., Gao, J., Zheng, J., Anderson, C. T., Jia, S., Wang, X., Cheng, W. H., Sengupta, S. et al. (2008). Prestin-based outer hair cell motility is necessary for mammalian cochlear amplification. *Neuron* **58**, 333-339.
Davies, C., Tingley, D., Kachar, B., Wenthold, R. J. and Petralia, R. S. (2001). Distribution of members of the PSD-95 family of MAGUK proteins at the synaptic region of inner and outer hair cells of the guinea pig cochlea. *Synapse* **40**, 258-268.
Duckert, L. G. and Rubel, E. W. (1990). Ultrastructural observations on regenerating hair cells in the chick basilar papilla. *Hear. Res.* **48**, 161-182.
Duckert, L. G. and Rubel, E. W. (1993). Morphological correlates of functional recovery in the chicken inner ear after gentamycin treatment. *J. Comp. Neurol.* **331**, 75-96.
Feng, A. S., Narins, P. M., Xu, C.-H., Lin, W.-Y., Yu, Z.-L., Qiu, Q., Xu, Z.-M. and Shen, J.-X. (2006). Ultrasonic communication in frogs. *Nature* **440**, 333-336.
Fettiplace, R. (2006). Active hair bundle movements in auditory hair cells. *J. Physiol.* **576**, 29-36.
Gale, J. E., Meyers, J. R., Periasamy, A. and Corwin, J. T. (2002). Survival of bundleless hair cells and subsequent bundle replacement in the bullfrog's saccule. *J. Neurobiol.* **50**, 81-92.
Gale, J. E., Piazza, V., Ciubotaru, C. D. and Mammano, F. (2004). A mechanism for sensing noise damage in the inner ear. *Curr. Biol.* **14**, 526-529.
Haque, A., Zakir, M. and Dickman, J. D. (2009). Regeneration of vestibular horizontal semicircular canal afferents in pigeons. *J. Neurophysiol.* **102**, 1274-1286.
Harding, G. W. and Bohne, B. A. (2004a). Noise-induced hair-cell loss and total exposure energy: analysis of a large data set. *J. Acoust. Soc. Am.* **115**, 2207-2220.
Harding, G. W. and Bohne, B. A. (2004b). Temporary DPOAE level shifts, ABR threshold shifts and histopathological damage following below-critical-level noise exposures. *Hear. Res.* **196**, 94-108.
Hordichok, A. J. and Steyger, P. S. (2007). Closure of supporting cell scar formations requires dynamic actin mechanisms. *Hear. Res.* **232**, 1-19.
Hudspeth, A. J., Choe, Y., Mehta, A. D. and Martin, P. (2000). Putting ion channels to work: mechanoelectrical transduction, adaptation, and amplification by hair cells. *Proc. Natl. Acad. Sci. USA* **97**, 11765-11772.
Kemp, D. T. (1978). Stimulated acoustic emissions from within the human auditory system. *J. Acoust. Soc. Am.* **64**, 1386-1391.
Kemp, D. T. (2002). Otoacoustic emissions, their origin in cochlear function, and use. *Br. Med. Bull.* **63**, 223-241.
Kornau, H. C., Schenker, L. T., Kennedy, M. B. and Seeburg, P. H. (1995). Domain interaction between NMDA receptor subunits and the postsynaptic density protein PSD-95. *Science* **269**, 1737-1740.
Kössl, M. and Boyan, G. S. (1998). Otoacoustic emissions from a nonvertebrate ear. *Naturwissenschaften* **85**, 124-127.
Kössl, M. and Vater, M. (1996). Further studies on the mechanics of the cochlear partition in the mustached bat. II. A second cochlear frequency map derived from acoustic distortion products. *Hear. Res.* **94**, 78-86.
Lewis, E. R. (1976). Comparative scanning electron microscopy study of the anuran basilar papilla. *Ann. Proc. Electron Microsc. Soc. Am.* **35**, 632-633.
Lewis, E. R. (1984). On the frog amphibian papilla. *Scan. Electron Microsc.* **4**, 1899-1913.
Lewis, E. R. and Li, C. W. (1975). Hair cell types and distributions in the otolithic and auditory organs of the bullfrog. *Brain Res.* **83**, 35-50.
Liberman, M. C., Zuo, J. and Guinan, J. J. J., Jr (2004). Otoacoustic emissions without somatic motility: can stereocilia mechanics drive the mammalian cochlea? *J. Acoust. Soc. Am.* **116**, 1649-1655.
Lonsbury-Martin, B. L., McCoy, M. J., Whitehead, M. L. and Martin, G. K. (1993). Clinical testing of distortion-product otoacoustic emissions. *Ear Hear.* **14**, 11-22.
Maison, S. F., Vetter, D. E. and Liberman, M. C. (2007). A novel effect of cochlear efferents: in vivo response enhancement does not require alpha9 cholinergic receptors. *J. Neurophysiol.* **97**, 3269-3278.
Mauermann, M. and Kollmeier, B. (2004). Distortion product otoacoustic emission (DPOAE) input/output functions and the influence of the second DPOAE source. *J. Acoust. Soc. Am.* **116**, 2199-2212.
Meenderink, S. W. F. and van Dijk, P. (2004). Level dependence of distortion product otoacoustic emissions in the leopard frog, *Rana pipiens pipiens*. *Hear. Res.* **192**, 107-118.
Meenderink, S. W. F. and van Dijk, P. (2006). Temperature dependence of anuran distortion product otoacoustic emissions. *J. Assoc. Res. Otolaryngol.* **7**, 246-252.
Meenderink, S. W. F., van Dijk, P. and Narins, P. M. (2005). Comparison between distortion product otoacoustic emissions and nerve fiber responses from the basilar papilla of the frog. *J. Acoust. Soc. Am.* **117**, 3165-3173.
Mills, D. M. (2004). Relationship of neural and otoacoustic emission thresholds during endocochlear potential development in the gerbil. *J. Acoust. Soc. Am.* **116**, 1035-1043.
Narins, P. M. and Hurley, D. D. (1982). The relationship between call intensity and function in the puerto rican coqui (Anura: Leptodactylidae). *Herpetologica* **38**, 287-295.
Narins, P. M. and Wagner, I. (1989). Noise susceptibility and immunity of phase locking in amphibian auditory-nerve fibers. *J. Acoust. Soc. Am.* **85**, 1255-1265.
Narins, P. M. and Zelick, R. (1988). The effects of noise on auditory processing and behavior in amphibians. In *The Evolution of the Amphibian Auditory System* (ed. B. Fritzsch, M. J. Ryan, W. Wilczynski, T. E. Hetherington and W. Walkowiak), pp. 511-536. New York, NY: John Wiley & Sons.
Narins, P. M., Ehret, G. and Tautz, J. (1988). Accessory pathway for sound transfer in a neotropical frog. *Proc. Natl. Acad. Sci. USA* **85**, 1508-1512.
Ohlms, L. A., Lonsbury-Martin, B. L. and Martin, G. K. (1991). Acoustic-distortion products: separation of sensory from neural dysfunction in sensorineural hearing loss in human beings and rabbits. *Otolaryngol. Head Neck Surg.* **104**, 159-174.
Peng, A. W. and Ricci, A. J. (2011). Somatic motility and hair bundle mechanics, are both necessary for cochlear amplification? *Hear. Res.* **273**, 109-122.
Prieve, B. A. (2002). Otoacoustic emissions in neonatal screening. In *Otoacoustic Emissions – Clinical Applications*, 2nd edn (ed. M. S. Robinette and T. J. Glattke), pp. 348-374. New York, NY: Thieme.
Reng, D., Müller, M. and Smolders, J. W. (2001). Functional recovery of hearing following ampa-induced reversible disruption of hair cell afferent synapses in the avian inner ear. *Audiol. Neurootol.* **6**, 66-78.
Ryals, B. M. and Westbrook, E. W. (1994). TEM analysis of neural terminals on autoradiographically identified regenerated hair cells. *Hear. Res.* **72**, 81-88.

Shera, C. A. and Guinan, J. J. J., Jr (1999). Evoked otoacoustic emissions arise by two fundamentally different mechanisms: a taxonomy for mammalian OAEs. *J. Acoust. Soc. Am.* **105**, 782-798.
Shofner, W. P. and Feng, A. S. (1983). A quantitative light microscopic study of the bullfrog amphibian papilla tectorium: correlation with the tonotopic organization. *Hear. Res.* **11**, 103-116.
Simmons, D. D., Meenderink, S. and Vassilakis, P. N. (2007). Anatomy, physiology, and function of auditory end-organs in the frog inner ear. In *Hearing and Sound Communication in Amphibians* (ed. P. M. Narins, A. S. Feng and A. N. Popper), pp. 184-220. New York, NY: Springer-Verlag.
Smotherman, M. S. and Narins, P. M. (2000). Hair cells, hearing and hopping: a field guide to hair cell physiology in the frog. *J. Exp. Biol.* **203**, 2237-2246.
Sobkowicz, H. M., Loftus, J. M. and Slapnick, S. M. (1993). Tissue culture of the organ of Corti. *Acta Otolaryngol. Suppl.* **502**, 3-36.
Sobkowicz, H. M., August, B. K. and Slapnick, S. M. (1997). Cellular interactions as a response to injury in the organ of Corti in culture. *Int. J. Dev. Neurosci.* **15**, 463-485.
van Dijk, P. and Manley, G. A. (2001). Distortion product otoacoustic emissions in the tree frog *Hyla cinerea*. *Hear. Res.* **153**, 14-22.
van Dijk, P., Narins, P. M. and Mason, M. J. (2003). Physiological vulnerability of distortion product otoacoustic emissions from the amphibian ear. *J. Acoust. Soc. Am.* **114**, 2044-2048.
van Dijk, P., Mason, M. J., Schoffelen, R. L. M., Narins, P. M. and Meenderink, S. W. F. (2011). Mechanics of the frog ear. *Hear. Res.* **273**, 46-58.
Vassilakis, P. N., Meenderink, S. W. F. and Narins, P. M. (2004). Distortion product otoacoustic emissions provide clues hearing mechanisms in the frog ear. *J. Acoust. Soc. Am.* **116**, 3713-3726.
Whitlon, D. S. and Sobkowicz, H. M. (1991). Patterns of hair cell survival and innervation in the cochlea of the bronx waltzer mouse. *J. Neurocytol.* **20**, 886-901.
Xiang, M. L., Mu, M. Y., Pao, X. and Chi, F. L. (2000). The reinnervation of regenerated hair cells in the basilar papilla of chicks after kanamycin ototoxicity. *Acta Otolaryngol.* **120**, 912-921.
Zakir, M. and Dickman, J. D. (2006). Regeneration of vestibular otolith afferents after ototoxic damage. *J. Neurosci.* **26**, 2881-2893.
Zelick, R. and Narins, P. M. (1985). Temporary threshold shift, adaptation, and recovery characteristics of frog auditory nerve fibers. *Hear. Res.* **17**, 161-176.
Zheng, Q. Y., Johnson, K. R. and Erway, L. C. (1999). Assessment of hearing in 80 inbred strains of mice by ABR threshold analyses. *Hear. Res.* **130**, 94-107.